

Two Classes of Visual Motion Sensitive Interneurons Differ in Direction and Velocity Dependency of *in Vivo* Calcium Dynamics

Volker Dürr,* Rafael Kurtz, Martin Egelhaaf

Lehrstuhl für Neurobiologie, Fakultät für Biologie, Universität Bielefeld, Postfach 10 01 31, D-33501 Bielefeld, Germany

Received 5 June 2000; accepted 1 November 2000

ABSTRACT: Neurons exploit both membrane biophysics and biochemical pathways of the cytoplasm for dendritic integration of synaptic input. Here we quantify the tuning discrepancy of electrical and chemical response properties in two kinds of neurons using *in vivo* visual stimulation. Dendritic calcium concentration changes and membrane potential of visual interneurons of the fly were measured in response to visual motion stimuli. Two classes of tangential cells of the lobula plate were compared, HS-cells and CH-cells. Both neuronal classes are known to receive retinotopic input with similar properties, yet they differ in morphology, physiology, and computational context. Velocity tuning and directional selectivity of the electrical and calcium responses were investigated. In both cell classes, motion-induced calcium accumulation did not follow the early transient of the membrane potential. Rather, the amplitude of the calcium signal seemed to be related to the late component of the depolarization, where it was close to a steady state. Electrical and calcium responses differed

with respect to their velocity tuning in CH-cells, but not in HS-cells. Furthermore, velocity tuning of the calcium response, but not of the electrical response differed between neuronal classes. While null-direction motion caused hyperpolarization in both classes, this led to a calcium decrement in CH-cells, but had no effect on the calcium signal in HS-cells, not even when calcium levels had been raised by a preceding excitatory motion stimulus. Finally, the voltage- $[Ca^{2+}]_i$ -relationship for motion-induced, transient potential changes was steeper and less rectifying in CH-cells than in HS-cells. These results represent an example of dendritic information processing *in vivo*, where two neuronal classes respond to identical stimuli with a similar electrical response, but differing calcium response. This highlights the capacity of neurons to segregate two response components.

© 2001 John Wiley & Sons, Inc. *J Neurobiol* 46: 289–300, 2001

Keywords: chemical computation; visual interneuron; calcium accumulation; directional selectivity; dendritic information processing; lobula plate; fly

INTRODUCTION

With their seminal work on the computational role of dendritic calcium concentration changes in neuronal information processing, Sobel and Tank (1994) made a

case for “chemical computation.” According to this concept, biochemically active ions and molecules are not only messengers in signaling pathways, but are part of an interactive framework connecting the cytoplasm with the cell membrane. In the case of calcium ions, these interactions can work in both ways, i.e., ion concentration changes depending on electrical activity and vice versa. Therefore, chemical and electrical response components both play a causal role in shaping the spatio-temporal activity pattern of a neuron, and both need to be monitored in order to understand its dendritic integration properties.

*Present address: Abteilung für Biologische Kybernetik und Theoretische Biologie, Fakultät für Biologie, Universität Bielefeld, Postfach 10 01 31, D-33501 Bielefeld, Germany.

Correspondence to: V. Dürr (volker.duerr@biologie.uni-bielefeld.de).

Contract grant sponsor: Deutsche Forschungsgemeinschaft, DFG.

Voltage-dependent calcium influx in dendrites appears to be a general feature of both vertebrate and invertebrate neurons (Regehr and Tank, 1994; Borst and Egelhaaf, 1994), and several functional roles of intracellular calcium in neurons have been proposed (Kostyuk, 1992). To date, only a few studies on dendritic calcium accumulation have been based on sensory stimulation *in vivo* (e.g., Borst and Egelhaaf, 1992; Sobel and Tank, 1994; Egelhaaf and Borst, 1995; Ogawa et al., 1996; Single and Borst, 1998; Dürr and Egelhaaf, 1999). As a result, we still know very little about the neural transformation of an electrical input pattern into a calcium ion distribution under real world conditions. Also, in spite of rather detailed knowledge about the biophysics of particular neurons, differences in animal preparation, stimulus protocol, network organization, and computational task often complicate transfer of experimental results from one type of neuron to another. The present study attempts to overcome this problem by comparing the responses of two kinds of neurons in the same model system, the visual system of the blowfly *Calliphora erythrocephala*. Calcium and electrical response components to identical stimuli are monitored in an *in vivo* preparation of two classes of individually identified interneurons: Centrifugal Horizontal cells (CH-cells) and cells of the Horizontal System (HS-cells).

These cell classes differ both in physiological features and in computational tasks. However, their anatomical vicinity, receptive field, directional selectivity, and local input-output characteristics (e.g. Egelhaaf et al., 1993; Kondoh et al., 1995) suggest that they receive similar input by pooling retinotopic information, possibly from the same set of ipsilateral elementary motion detectors (Egelhaaf and Borst, 1993). Therefore, dendritic calcium accumulation can be studied under identical stimulus conditions, and differences in the cellular responses are likely to reflect different cellular properties.

CH-cells (Eckert and Dvorak, 1983; Gauck et al., 1997) and HS-cells (Hausen, 1976; Hausen et al., 1980; Hausen, 1982a) belong to the tangential cells of the lobula plate, the posterior part of the third visual neuropil. Both cell classes are sensitive to large-field visual motion, and are strongly direction-selective for horizontal motion, such that they depolarize in response to front-to-back motion and hyperpolarize to back-to-front motion. In a behavioral context, tangential cells are thought to play a pivotal role in information processing of optic flow (Egelhaaf et al., 1988; Egelhaaf and Borst, 1993). HS-cells are output neurons of the lobula plate and are probably involved in mediating the optomotor response (Hausen and Wehrhahn, 1989; Hausen and Wehrhahn, 1990). In con-

trast, CH-cells relay ipsilateral input within the lobula plate via dendritic synapses (Gauck et al., 1997). They have been proposed to be involved in figure-ground-discrimination (Warzecha et al., 1993).

Recent comparative optical recording studies in the same model system revealed that calcium accumulation is faster in CH-cells than in HS-cells (Dürr and Egelhaaf, 1999; Haag and Borst, 2000). Furthermore, the spatial integration properties of CH- and HS-cells are known to differ (Dürr and Egelhaaf, 1999). The present study takes a comparative view of the dependency of dendritic $[Ca^{2+}]_i$ on stimulus velocity and direction of visual motion stimuli. Velocity is known to strongly affect dynamic components in the membrane potential of tangential cells (Egelhaaf and Borst, 1989), whereas directional selectivity of the electrical response, combined with a voltage-dependent calcium influx (Egelhaaf and Borst, 1995; Single and Borst, 1998), renders intracellular calcium accumulation an important mediator of input-output nonlinearities. Because flying insects may experience vigorous changes in velocity and direction of visual motion, the results provide helpful new insights into spatio-temporal processing of visual motion stimuli. In the context of chemical computation, the results highlight the opportunities of neurons to transform similar input information into differing, task-specific output.

MATERIALS AND METHODS

Animal preparation and electrophysiological and optical imaging methods have been described in detail by Dürr and Egelhaaf (1999), and will only be briefly reiterated here.

Preparation and Stimulus Procedure

Animals were anaesthetized with carbon dioxide and waxed to a glass support. The head was pitched to face downward. Then, the right lobula plate was exposed, such that it was visible under an epifluorescence microscope (Zeiss Universal III-RS). The visual motion stimulus was presented from below, by projection of two stripe patterns ($\emptyset 66^\circ$) onto an opaque sphere (ca. 33° spatial wavelength, equivalent to 0.03 cycles/degree; 68% contrast; 12 cd/m² mean light intensity). Luminance (Hausen, 1981) and contrast (Egelhaaf and Borst, 1989) of the stimulus were in a range where electrical responses of tangential cells did not depend much on these parameters, but they were well within the natural working range of the fly visual system (Egelhaaf et al., 2000). The spectral composition of the stimulus was that of a Hg-arc-lamp (Osram HBO 100W) with wavelengths between 450 and 700 nm filtered out by a blue filter (BG1, Schott). Filtering helped to minimize light transmission

through the head of the animal and, thus, interference with the fluorescence light emanating from the dyed cell. The visual stimulus could be adjusted to match the receptive field and preferred direction of the recorded visual interneuron.

The angular velocity of the moving pattern was set to 16.5, 66, 264, or 792°/s, corresponding to a temporal frequency of 0.5, 2, 8, or 24 Hz. For reasons of comparison with earlier work, velocity of visual motion will be expressed as temporal frequency throughout this study.

Three kinds of stimulus protocols were used. The “excitation protocol” consisted of 2 s pattern motion in the preferred-direction at one of the four velocities, preceded by a 2 s pre-excitation phase and followed by a 2 s post-excitation phase with no pattern motion. The “inhibition protocol” was the same, except that stimulus direction was inverted to the null-direction of the cell. In an “excitation-inhibition protocol,” excitation was achieved by a 2 Hz motion stimulus in the preferred-direction and subsequent inhibition by null-direction motion at either 2 or 8 Hz temporal frequency.

Electrical recordings were acquired either during dye injection with weak tonic hyperpolarization (0.4–1.5 nA) or during optical recording. In the first case, a random sequence of the four excitation and the two excitation-inhibition protocols was used, each one presented three times. During optical recording, single presentations of any protocol were used, each one followed by a further 2 s period of no pattern motion.

Electrophysiology and Optical Imaging

The cells were intracellularly recorded, using sharp glass electrodes (GC100F-10, Clark) pulled on a Brown-Flaming puller (P80-PC or P97, Sutter Instruments). When filled with 1 M KCl, their resistance was 30–40 M Ω . The indifferent electrode was a wide-tip glass pipette, also used for supplying the preparation with Ringer-solution. Voltage was recorded by an Axoclamp-2A amplifier (Axon Instruments) in bridge-mode, low-pass filtered at 2 kHz, AD-converted at an amplitude resolution of 0.0244 mV per count (DT2801A, Data Translation), and stored on a computer (IBM-AT). Data were sampled at 1 kHz and stored as single traces or as averaged traces of three recordings. Computer programs for stimulus control, electrophysiology, and data analysis were written in Turbo Pascal (Borland; some TP-units were kindly supplied by R. Feiler, MPI für biologische Kybernetik in Tübingen, Germany). Except for data in Figure 4(B), all presented electrical recordings were made independent of the optical recordings, but with exactly the same stimulus conditions. Statistical tests were calculated using the Statistics Package for the Social Sciences 8.0 (SPSS Inc.).

Changes in intracellular ionic calcium concentration $[Ca^{2+}]_i$ were measured as relative fluorescence changes, $\Delta F/F$, of the intracellular calcium-sensitive dye Fura-2 (Fura-2 pentapotassium salt, 20 mM, Molecular Probes;

KCl, 33.3 mM, KOH, 1.7 mM, Merck; HEPES, 33.3 mM, Sigma; pH 7.3).

The imaging system consisted of a Hg-arc lamp (HBO 100 W, Osram), a 380 nm excitation filter, a 490 nm dichroic mirror, a 500–530 barrier filter, and a Photometrics PXL camera system connected to a PC. For image acquisition and processing the software package PMIS (GKRCC) was used. Temporal resolution of all measurements was 3 Hz with 128 \times 128 pixel images and 290 ms exposure. Spatial resolution was 9 μ m.

$\Delta F/F$ was calculated from single-wavelength measurements (Vranesic and Knöpfel, 1991) with reference to the second image of the series. $\Delta F/F$ values were inverted in order to describe increments of $[Ca^{2+}]_i$ with positive $\Delta F/F$ -values. Both the resting fluorescence in the cell and its underlying background fluorescence, two essential parameters for single-wavelength measurement of $\Delta F/F$, change across the neuropil. Because the exact background fluorescence underneath a given dyed dendrite cannot be determined, and the exact match of a certain dendritic region cannot be found from one preparation to another, we chose to analyze the mean $\Delta F/F$ across the entire dendritic arborization in the lobula plate (see images in Fig. 1). This procedure ensured consistent choice of the analyzed dendritic region, which is the basis for a quantitative comparative study. Background fluorescence was determined in an image region away from the dyed neuron. This image region remained the same for all measurements of a given cell, and background fluorescence was determined separately in each frame. For further details on image analysis see Dürr and Egelhaaf (1999) or Dürr (1998).

RESULTS

Velocity Dependency Differs between Electrical and Calcium Responses

Motion-induced depolarization in CH- and HS-cells exhibits a transient early component and a late component where depolarization reaches a steady state (Hausen, 1982b). The time course of the response depends on the stimulus conditions. In particular, the amplitude of the early transient response component of lobula plate tangential cells is strongly affected by stimulus velocity (Maddess and Laughlin, 1985; Egelhaaf and Borst, 1989). In order to investigate the extent to which the transient response component affects calcium accumulation, we recorded both electrical and calcium responses to pattern motion in the preferred-direction of the cell at four different velocities (Fig. 1). During the 2-s stimulus period used in this study, depolarization did not always reach a steady state, although early and late components were clearly discernible (Fig. 1). Within the tested velocity range, the amplitude ratio of early and late components increased in both cell classes from 1.2–1.5 at 2

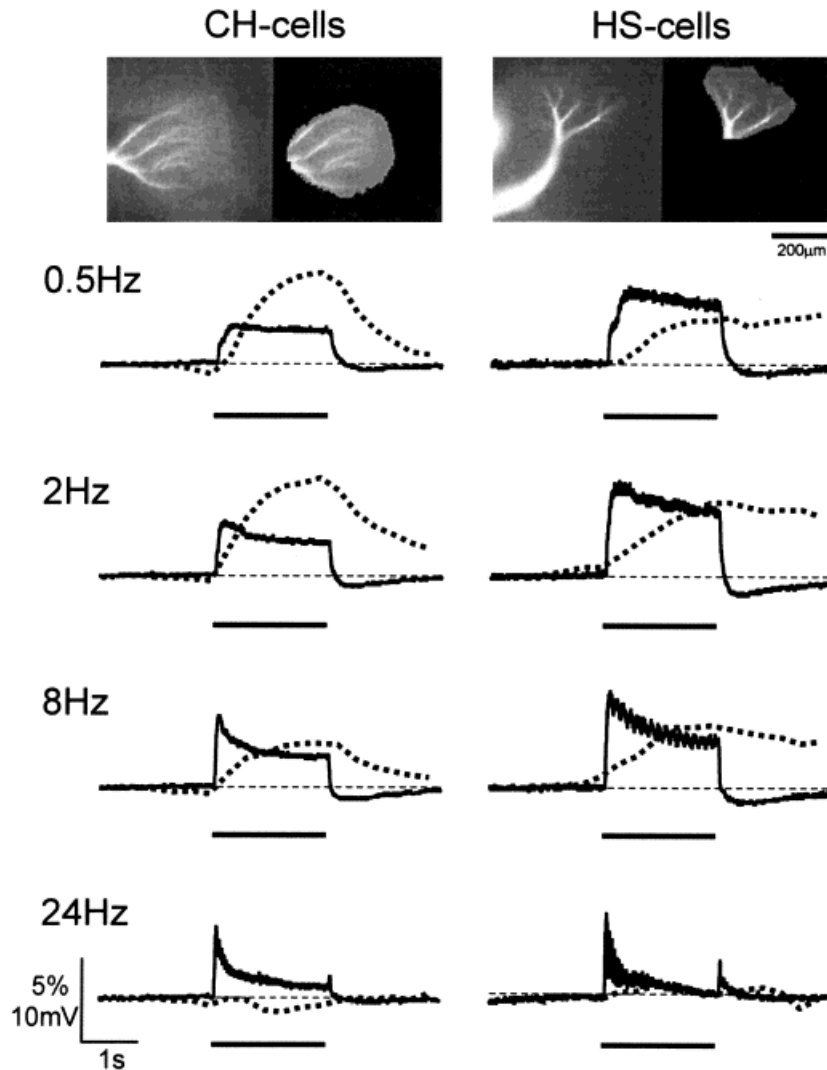


Figure 1 Electrical and calcium responses to different stimulus velocities. Raw fluorescence images show the ventral Centrifugal Horizontal cell (CH-cell) and the northern cell of the Horizontal System (HS-cell), both of which have extensive dendritic arborizations in the lobula plate. Juxtaposed images display the same images with the mask delimiting the analyzed region. For reasons of quantitative comparability, the analyzed region was defined as the entire region located between the major dendrites. Diagrams show averaged changes in membrane potential (ΔE_M , solid lines) and calcium concentration ($\Delta F/F$, dotted lines) of CH- and HS-cells in response to motion stimuli with four different pattern velocities. Velocity is given as the temporal frequency of the moving stripe pattern. Traces were averaged from mean cell responses. Numbers of sweeps and cells (in parentheses): electrical response CH: 123(27); HS: 111(30); calcium response CH: 0.5 Hz 32(9), 2 Hz 59(10), 8 Hz 38(10), 24 Hz 21(9); HS: 0.5 Hz 12(7), 2 Hz 21(8), 8 Hz 11(5), 24 Hz 6(4). Horizontal bars below the traces depict the stimulus period. The shoulder in the rising phase of the depolarization to 0.5 Hz motion is an artifact due to the mechanical backlash of the stimulus. At all higher velocities, the effect of this slip was negligible.

Hz to more than 3.0–3.8 at 24 Hz (early component: 200 ms window, starting 100 ms after stimulus onset; late component: 1000 ms window, 1000 ms after stimulus onset). At high velocities, particularly in HS-cells, membrane depolarization is modulated with the temporal frequency of the stimulus. When pattern

motion stops, the membrane potential exhibits an after-response that is hyperpolarizing at low velocities, but reverses sign to become depolarizing at the highest tested velocity. As a recent study by Kurtz et al. (2000) specifically addresses the appearance of this depolarizing off-response in relation to a putative

calcium-induced mechanism of motion adaptation, we will not consider it further here. In contrast to the membrane potential, the corresponding mean calcium response across the dendrite increases only slowly. Even at high velocities, in response to which membrane depolarization becomes highly transient, there is no observable calcium transient. Rather, it is the late component of the electrical response that appears to be reflected in the amplitude of the calcium response. Slow calcium accumulation was not simply a consequence of low sampling frequency, because much faster fluorescence measurements, using a photodiode, result in similarly slow dendritic calcium accumulation (Egelhaaf and Borst, 1995). A further methodical pitfall that could slow down the calcium response is calcium buffering by the dye itself (e.g., Tank et al., 1995). Although dye affinity, and thus the buffering effect, of the calcium indicator itself is known to alter calcium kinetics in tangential cells, Haag and Borst (2000) recorded calcium accumulation with a long time constant even with low-affinity dyes. Their results suggest that dye affinity is not sufficient to cause the slow time course of calcium accumulation.

Figure 1 shows that variation of stimulus velocity greatly alters the dynamic properties of the electrical response, but not of the concurrent calcium response. Thus, calcium accumulation resembles a low-pass filtered version of the depolarization time course. As has been described before (Dürr and Egelhaaf, 1999), CH-cells exhibit faster increase and decrease of $[Ca^{2+}]_i$ than HS-cells. Furthermore, neither cell class exhibits a calcium after-response other than a slow decrease of $[Ca^{2+}]_i$ to its resting level.

Quantitative comparison of electrical and calcium velocity tuning is displayed in Figure 2 and the corresponding statistical values are listed in Table 1. In order to compare both response parameters and both cell classes, the late component of the electrical response and the mean calcium response were determined for individual cells and normalized with respect to the median of the 2 Hz-response. The velocity tuning of the electrical signal is not statistically different between the two cell classes (Mann-Whitney test; $p > .95$). In the calcium response, however, HS-cells exhibit significantly weaker responses to the 0.5 Hz-stimulus compared to CH-cells ($p = .005$). Comparison of matched pairs of electrical and calcium responses yields a significant difference in CH-cells for the 24 Hz-stimulus (Wilcoxon's rank test; $p = .018$), but no difference in HS-cells. In order to discern possible trends in the data, we suggest a second, weaker statistical criterion. Wherever the boxes of the box-whisker plots in Figure 2 do not

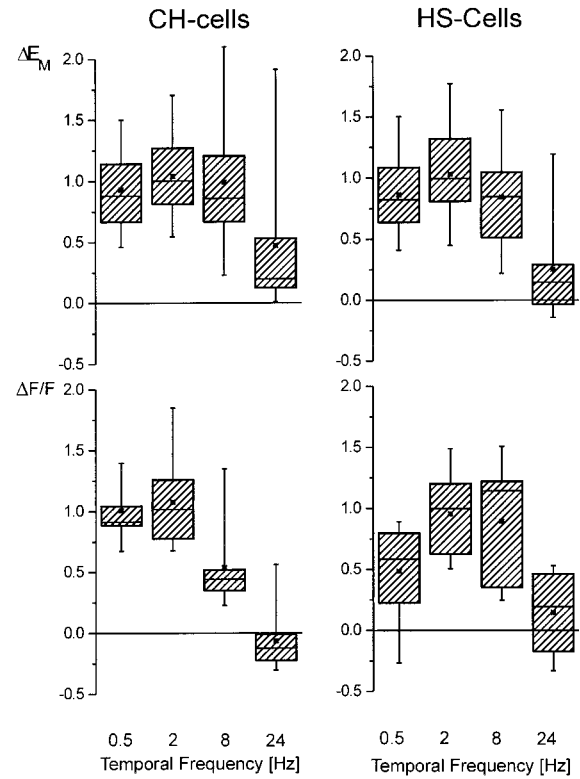


Figure 2 Temporal frequency dependency of calcium and electrical responses. Box-whisker plots show distributions of mean cell responses. ΔE_M is the late component of the depolarization, determined in a 1 s window 1 s after stimulus onset. $\Delta F/F$ is the mean relative fluorescence change during the stimulus period. Both responses were normalized with respect to the median response to the 2 Hz stimulus (median ΔE_M : CH 4.6 mV, HS 8.4 mV; median $\Delta F/F$: CH 4.22%, HS 3.09%). The middle 50% percent of the data values are comprised by the box. The horizontal line dividing the box marks the value of the median. Star symbols indicate the arithmetic mean. Whiskers show 5%- and 95%-percentiles, i.e., the range comprising 90% of the data. Sample sizes are given in the first two lines of Table 1.

overlap, at least 75% of each sample distribution do not overlap with the other, i.e., 75% of the values are smaller or larger than the entire compared distribution. Applying this criterion reveals that in CH-cells, but not in HS-cells, the calcium response is more attenuated than the electrical response for both the 8 and 24 Hz conditions (Table 1). According to both criteria, velocity tuning of the electrical response does not differ between the cell classes, whereas the calcium response does. Also, in CH-cells, calcium responses tend to attenuate more than concurrent electrical responses at high pattern velocities. In five out of seven preparations, a 24 Hz-stimulus caused a decrease of $[Ca^{2+}]_i$ in spite of concurrent depolarization.

Table 1 Statistical Values of Velocity Tuning Results Displayed in Figure 2

Null Hypothesis	0.5 Hz	2 Hz	8 Hz	24 Hz
$H_0: El_{CH} = El_{HS}$	0.511 $n_1 = 26$ $n_2 = 30$	0.895 $n_1 = 26$ $n_2 = 30$	0.430 $n_1 = 26$ $n_2 = 30$	0.079 $n_1 = 26$ $n_2 = 30$
$H_0: Ca_{CH} = Ca_{HS}$	0.005* [†] $n_1 = 9$ $n_2 = 7$	0.573 $n_1 = 10$ $n_2 = 8$	0.440 $n_1 = 10$ $n_2 = 5$	0.604 $n_1 = 9$ $n_2 = 4$
$H_0: El_{CH} = Ca_{CH}$	0.249 $n = 6$	0.272 $n = 12$	0.124 [†] $n = 8$	0.018* [†] $n = 7$
$H_0: El_{HS} = Ca_{HS}$	0.091 $n = 7$	0.469 $n = 19$	0.225 $n = 5$	0.273 $n = 4$

Exact two-sided p -values and sample numbers are given for Mann-Whitney tests for differences of electrical and calcium responses (El and Ca, respectively) between cell classes ($n_1 =$ CH-cells and $n_2 =$ HS-cells), and Wilcoxon's rank tests on matched pairs for differences between electrical and calcium responses within a given cell class. Null hypotheses are listed in the leftmost column. Results marked by a [†] are distinguished by nonoverlapping 75% of data (see text). A star indicates significance at $p < .05$.

The results presented in Figure 2 demonstrate that visual interneurons may respond to identical visual stimulation with similar velocity tuning of the electrical response component, but a differing velocity tuning of the chemical response component.

Null-Direction Motion Reduces $[Ca^{2+}]_i$ in CH-Cells but Not in HS-Cells

Motion in the null-direction has been previously shown to have no effect on $[Ca^{2+}]_i$ in the major dendritic branches of HS-cells (Egelhaaf and Borst, 1995). However, because recent results of Single and Borst (1998) show that null-direction motion may cause local decrements of dendritic $[Ca^{2+}]_i$ in HS-cells, we tested whether such local decrements add up to an overall $[Ca^{2+}]_i$ change, when measured across the entire dendritic arbor (for evaluated dendritic area see Fig. 1). Figure 3(A) shows that this is not the case. Rather, motion-induced hyperpolarization of HS-cells does not cause a significant net change of $[Ca^{2+}]_i$ in the dendritic arbor. Although individual traces may show a motion-induced decrement of $[Ca^{2+}]_i$, this effect is prone to considerable variability.

Even if null-direction motion does not cause $[Ca^{2+}]_i$ to decrease below its resting concentration, it might well have an effect on its decline rate after experimentally increasing $[Ca^{2+}]_i$ by preferred-direction motion. We tested this hypothesis, using the excitation-inhibition protocol. Following the 2 s excitation phase, the membrane potential was quickly hyperpolarized (Fig. 3(B)). This motion-induced hyperpolarization was about four times stronger than the after-hyperpolarization observed without null-direction motion (Fig. 3(B): -4.55 and -4.09 mV for null-direction motion at 2 and 8 Hz, respectively, compared to -1.15 mV at no motion). The calcium responses to the three conditions are shown in Figure 3(C), where mean $\Delta F/F$ values were calculated for four subsequent 2 s bins (no motion, excitation, 2 times inhibition; see inset). In the excitation bin (Bin 2) and in both inhibition bins (Bins 3 and 4) the $\Delta F/F$

values vary between conditions (darker shading for faster null-direction motion). However, in none of the bins were observed differences between responses with and without null-direction motion statistically significant (Mann-Whitney test; $p > .9$). Thus, hyperpolarization induced by null-direction motion has no significant effect on $[Ca^{2+}]_i$, neither at resting nor at raised calcium levels (Fig. 3).

Whereas null-direction motion caused no $[Ca^{2+}]_i$ decrement in HS-cells, it did in CH-cells (Fig. 4(A)). In CH-cells, the $\Delta F/F$ time course during null-direction motion was similar to the time course during preferred-direction motion in that it did not follow fast changes in membrane potential. Plotting the voltage- $[Ca^{2+}]_i$ relationship for simultaneous recordings of calcium accumulation and membrane depolarization revealed an almost linear voltage- $[Ca^{2+}]_i$ relationship (Fig. 4(B)). To give a mathematical approximation of this relationship, a linear regression was calculated, which yielded the function $\Delta F/F = 0.788 \Delta E_M + 0.682$, and a correlation coefficient $r = 0.871$.

In summary, although both cell classes show pronounced hyperpolarization in response to null-direction motion (Fig. 3(A), Fig. 4(B)), HS-cells do not respond with an overall decrement of dendritic $[Ca^{2+}]_i$ (Fig. 3(B,C)), whereas CH-cells do (Fig. 4).

Voltage- $[Ca^{2+}]_i$ Relationships in CH- and HS-Cells during Brief, Phasic-Tonic Potential Changes Differ in Slope and Rectification

In order to analyze the voltage- $[Ca^{2+}]_i$ relationship over a range of stimulus velocities, we plotted motion-induced calcium responses over their corresponding voltage change during the late response component in a total of 12 CH-cells and 17 HS-cells (Fig. 5). Responses to motion of all tested stimulus velocities were included.

In CH-cells, null-direction motion of all tested pattern velocities typically leads to decrements in $[Ca^{2+}]_i$ (Fig. 5). Preferred-direction motion caused

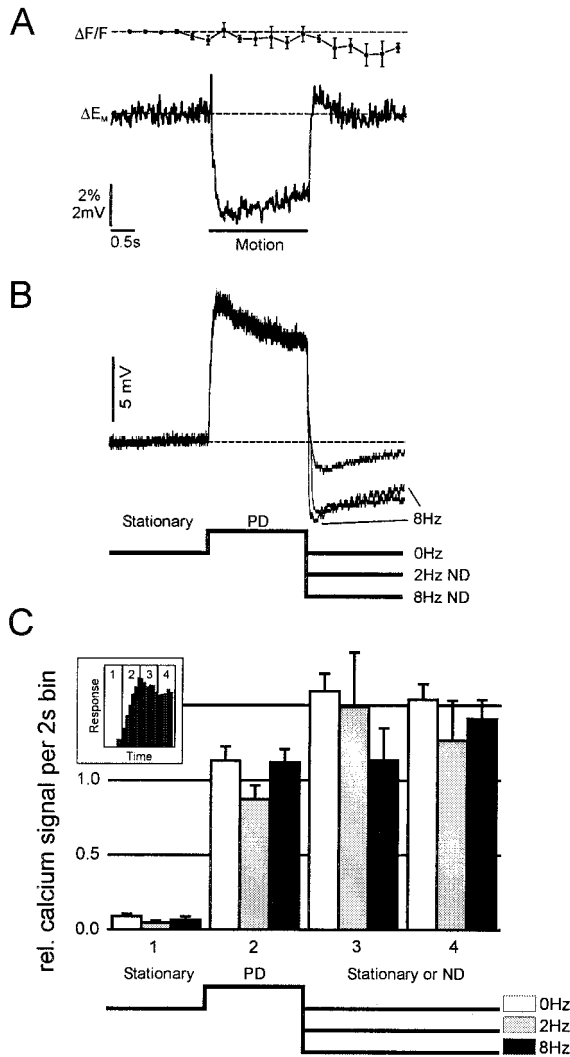


Figure 3 Null-direction motion does not change $[Ca^{2+}]_i$ in HS-cells. (A) Average response of four cells to null-direction (ND) motion at 2 Hz. There was no significant change of $\Delta F/F$ (top trace) due to hyperpolarization (bottom trace). Error bars denote S.E.M. (B) Average electrical responses of 33 HS-cells to ND-motion following depolarization during 2 s of preferred-direction (PD) motion. (C) Normalized calcium response amplitude in four subsequent 2 s bins (see inset) during excitation-inhibition experiments (see stimulation protocol beneath the figure). Following a 2 s excitation phase with motion in the PD at 2 Hz, the stimulus either stood still (white bars, $n = 8$), or was moving in the null-direction at 2 Hz (gray bars, $n = 6$) or 8 Hz (black bars, $n = 4$). Error bars show S.E.M. Each cell's response amplitude was normalized with respect to the cell's average $\Delta F/F$ value in response to a 2 Hz stimulus, and binned to the 2 s mean. Amplitudes were not statistically different according to a Mann-Whitney test for H_0 : effect of motion = effect of no motion. Inset: Representative example of a time course of calcium accumulation during the excitation-inhibition protocol. Black bars show individual $\Delta F/F$ measurements at 3 Hz temporal resolution. Bin spacing and numbering as used for (A) and (B) is indicated.

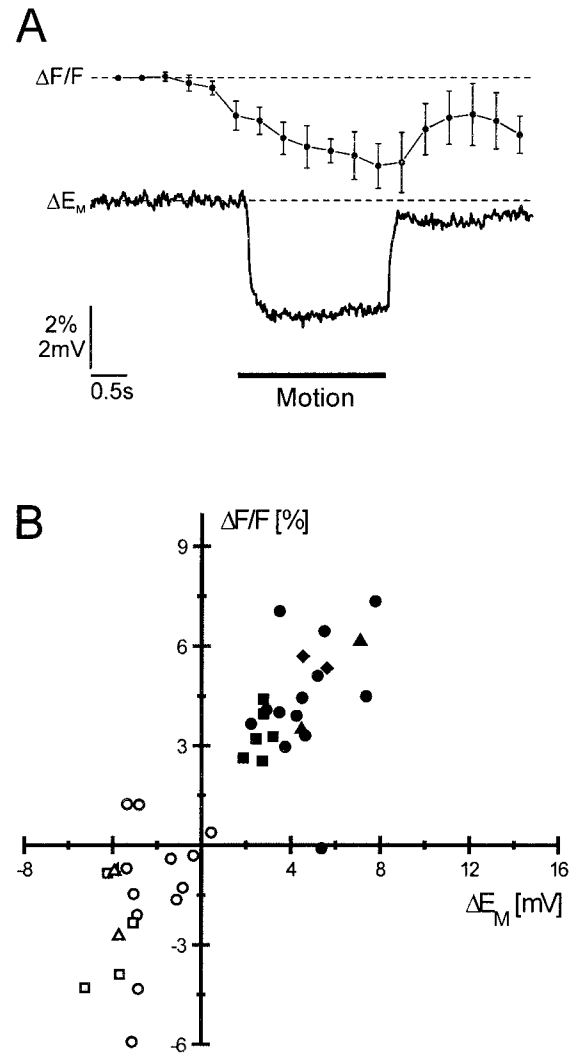


Figure 4 Null-direction motion causes decrements of $[Ca^{2+}]_i$ in CH-cells. (A) Null-direction motion at 2 Hz causes $[Ca^{2+}]_i$ to drop below resting level (top trace, $n = 4$) as well as hyperpolarization (bottom trace, $n = 6$). Same scale and graph details as Figure 3 (A). (B) Voltage- $[Ca^{2+}]_i$ relationship in simultaneous calcium and electrical recordings. Solid symbols for motion in preferred-direction, open symbols for motion in null-direction (both at 2 Hz). Different symbol shapes stand for different preparations. Data from four preparations, contributing 25, 10, 4, and 2 measurements.

calcium accumulation in most cases, except for responses to the 24 Hz-stimulus, where a calcium decrement was recorded in five out of seven preparations (see also Fig. 2). The voltage- $[Ca^{2+}]_i$ relationship of CH-cells for variable motion velocity thus appears slightly rectifying with a small negative offset. This is in agreement with the nearly linear dependency presented in Figure 4(B) (single pattern velocity), but

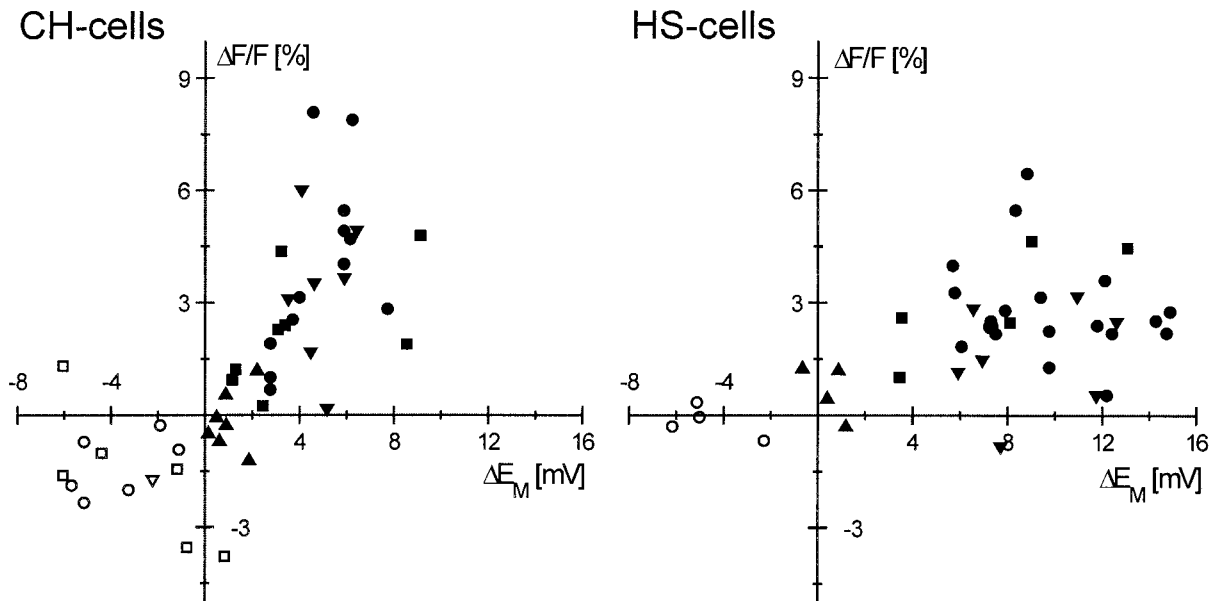


Figure 5 Voltage- $[Ca^{2+}]_i$ relationships in CH-cells and HS-cells. Mean cell responses to 2 s periods of stimulation with pattern motion at different temporal frequencies. Different symbols depict responses to different temporal frequencies: 0.5 Hz (down triangles), 2 Hz (circles), 8 Hz (squares), 24 Hz (up triangles). Solid and open symbols indicate motion in preferred- and null-direction, respectively. $\Delta F/F$ was calculated as the mean over the entire 2 s stimulus period. ΔE_M was the late component of the electrical response, i.e., the last of the two seconds. Linear fits for the data acquired during PD and ND motion gave the following slopes: CH 0.66 (PD), 0.23 (ND); HS 0.25 (PD), 0.02 (ND). Fits were fixed to the origin because zero motion causes neither an electrical nor a calcium response.

indicates that the ratio of calcium influx over potential change depends on motion velocity.

In HS-cells, significant changes in $[Ca^{2+}]_i$ were only observed in response to motion in the preferred-direction. The voltage- $[Ca^{2+}]_i$ relationship therefore was strongly rectifying (Fig. 5). Moreover, the slope of the relationship was shallower in HS-cells than in CH-cells, indicating that brief depolarizations, i.e., in the range of the time constant of dendritic calcium accumulation (Dürr and Egelhaaf, 1999) of a given amplitude have considerably weaker effect on intracellular calcium levels in HS-cells than in CH-cells.

DISCUSSION

Two classes of individually identified neurons in the insect visual system were compared with respect to their electrical and chemical (calcium) response components. As a prerequisite for quantitative comparison, identical visual motion stimuli were used to excite both kinds of cells *in vivo*. The overall dendritic calcium concentration change was measured along with the membrane potential in the axon. Chemical

and electrical response components were shown to differ in time course (Fig. 1), velocity tuning (Fig. 2), and directional selectivity (Figs. 3 and 4). Furthermore, the two cell classes revealed different voltage- $[Ca^{2+}]_i$ relationships (Fig. 5). In summary, the results demonstrate that different dendritic integration properties of neurons can remain concealed at the level of the membrane potential while being present at the level of calcium dynamics.

Earlier findings on HS- (Egelhaaf and Borst, 1995) and CH-cells (Dürr and Egelhaaf, 1999) indicated that calcium accumulation does not follow the transient changes in the membrane potential. Here we provide the first systematic account of this issue. First, stimulus parameters were specifically chosen to alter the ratio between early and late components of the electrical response. Second, for the sake of quantitative comparability between cells of a given class, and between cell classes with different arborization patterns and biophysical properties, we did not look at local changes in $[Ca^{2+}]_i$, but chose the overall signal for the entire dendritic arborization within the lobula plate (Fig. 1, see also Materials and Methods section). It was plausible to determine the mean dendritic cal-

cium accumulation rather than local concentration changes because the large-field motion stimuli excited a large portion of the dendritic arbor and the spatial distribution of voltage-gated calcium channels in these neurons is thought to be fairly even (Haag and Borst, 2000). Also, we relate the overall calcium signal to the membrane potential change at a single point in the axon.

Because functional interpretation of the presented results requires their discussion in the context of tangential cell physiology, the following sections will mainly draw connections between studies on the same model system. Nevertheless, most physiological considerations apply to neuronal dendrites in general. The following section will focus on the newly described discrepancy in velocity tuning. The final section is concerned with directional selectivity of the calcium response and the emergence of nonlinearities in the voltage- $[Ca^{2+}]_i$ relationship.

Velocity Tuning of Electrical and Calcium Responses

In the case of HS-cells, the velocity tuning of the electrical response (Fig. 2) is in agreement with earlier results by Hausen (1982b; Hausen and Wehrhahn, 1989), with a sharp drop of response amplitude for temporal frequencies above 10 Hz. The tuning of the calcium response was statistically indistinguishable from that of the electrical response. Egelhaaf and Borst (1995) reported a different location of the temporal frequency maximum for electrical and calcium response, i.e., calcium accumulation was still strong at 8 Hz temporal frequency, where the depolarization was much attenuated. The same study also displayed an HS-cell recording, where calcium accumulation was rather strong while concurrent steady state depolarization was close to zero. Although we occasionally recorded similarly strong calcium responses to a high-velocity motion stimulus, these responses were not representative in that they did not lead to a statistically detectable mismatch between electrical and calcium response in a larger sample of preparations. The large variability of the responses is reflected in the large whiskers in Figure 2 (denoting 5–95 percentile).

Temporal frequency tuning of CH-cells has never been published before. In this cell class, we found a difference in velocity tuning of electrical and calcium signals. This difference may be indicative of what has been termed chemical computation by Sobel and Tank (1994) in their *in vivo* study of the orthopteran auditory Ω -neuron. Although in CH-cells we do not know any concrete computational equivalent of the ob-

served tuning discrepancy, dendritic calcium is likely to act on inhibitory presynapses, which are known to exist in the dendrites of CH-cells (Gauck et al., 1997). In turn, this could lead to an altered velocity tuning in lobula plate neurons that are postsynaptic to CH-cells, compared to the tuning of their input elements.

Different velocity tuning of the two response components may be linked to the slower time course of the calcium response relative to the electrical response (Fig. 1). This is because a low-pass characteristic in the mechanism underlying calcium accumulation can cause increasing attenuation of local membrane potential oscillations with increasing temporal frequency of the stimulus. Tangential cells receive synaptically induced local membrane potential fluctuations at the frequency of local luminance fluctuations in the visual stimulus (Egelhaaf et al., 1989), which, in our case, is the temporal frequency of the periodic motion stimulus. These oscillations are a consequence of retinotopic input from local motion detectors (Egelhaaf and Borst, 1993). Retinotopy has been demonstrated by optical-recording experiments on HS- (Borst and Egelhaaf, 1992; Dürr and Egelhaaf, 1999) and CH-cells (Egelhaaf et al., 1993; Dürr and Egelhaaf, 1999). In accordance with these results, Single and Borst (1998) reported stimulus-induced local modulation of $[Ca^{2+}]_i$ at the temporal frequency of a slow motion stimulus in dendritic branches of HS-cells.

Directional Selectivity of Calcium Accumulation and Voltage- $[Ca^{2+}]_i$ Relationship

Because local phase-locking of calcium oscillations to retinotopic input modulation (Single and Borst, 1998) requires a fast Ca^{2+} efflux or a buffering mechanism to counteract the voltage-dependent Ca^{2+} influx, we used motion-induced hyperpolarization to investigate the voltage-dependence of calcium efflux. In our experiments, we found neither local nor overall decrements of $[Ca^{2+}]_i$ during null-direction motion in HS-cells. The lack of hyperpolarization-induced efflux of dendritic calcium in HS-cells (Fig. 3(B)) suggests that the dominant efflux mechanism is not voltage-dependent. This is in agreement with a result presented by Single and Borst (1998, their Fig. 4), where current injection as strong as -14 nA, resulting in at least five times the hyperpolarization amplitude of natural motion stimuli, failed to counterbalance motion-induced calcium accumulation in fine dendritic branches. The only part of an HS-neuron where Single and Borst recorded a $[Ca^{2+}]_i$ decline below resting level was the axon. In the axon, as in the dendrite, it took unnaturally strong hyperpolarization to induce a $[Ca^{2+}]_i$

decrement. These observations are in good agreement with a strongly rectifying voltage- $[Ca^{2+}]_i$ relationship in HS-cells (Fig. 5), according to which hyperpolarization of a given amplitude causes a smaller effect than a depolarization of the same amplitude.

Strong current injection into the axon of a CH-cell is known to cause a decrement of dendritic calcium, similar to the effect seen in HS-cells as described in the previous paragraph (Single, 1998; Haag and Borst, 2000). However, because passive membrane properties of CH-cells are thought to cause strong attenuation of an axonal potential step spreading into the dendrite (Borst and Haag, 1996; their Fig. 11), it is difficult to interpret this experimental condition. Haag and Borst (2000) demonstrated a synaptically driven drop in $[Ca^{2+}]_i$ comparable to our results in Figures 4 and 5, which give a more systematic and quantitative account on this finding. Our results demonstrate that motion-induced synaptic hyperpolarization of CH-cell dendrites can elicit a drop of $[Ca^{2+}]_i$ below resting level. Therefore, a voltage-dependent net Ca^{2+} -efflux must be postulated. Possible candidates underlying such a mechanism would be electrogenic Na^+/Ca^{2+} -exchangers in the outer cell membrane (review: Blaustein and Lederer, 1999). Alternatively, if there was an equilibrium of Ca^{2+} -influx and -efflux at resting membrane potential, hyperpolarization could shut down Ca^{2+} -influx through voltage-gated channels, leading to a net Ca^{2+} -efflux.

In a recent study on dendritic calcium accumulation in tangential cells, Dürr and Egelhaaf (1999) focused on the effect of stimulus size and contrast, the variation of which only mildly affected the time course of the electrical response. Normalization of the electrical and calcium signals to a reference stimulus condition revealed that HS-cells respond to contrast increments in a nonlinear fashion: Depolarization by low-contrast stimuli was relatively stronger than the concurrent calcium accumulation. CH-cells on the other hand, showed an approximately linear relationship. In comparison, the voltage- $[Ca^{2+}]_i$ relationship of CH-cells presented in Figure 4(B), where the same stimulus velocity was used as in the previous study, extends the earlier finding to hyperpolarized membrane potentials. However, the discrepancy of velocity tuning of calcium and electrical responses at high velocities (Fig. 2) requires a nonlinearity in the voltage- $[Ca^{2+}]_i$ relationship. Possibly, the explanation of this effect is linked to the weak directional tuning of the input elements to the tangential cells (Borst et al., 1995; Single et al., 1997). Because tangential cells pool excitatory and inhibitory synaptic inputs (Egelhaaf et al., 1990; Gilbert, 1990; Brotz and Borst, 1996), a certain membrane potential may be the result

of a particular balance of opposing inputs, mainly differing in the magnitude of their antagonistic inputs. Thus, if motion stimuli were to change both ratio and magnitude of antagonistic inputs, this could cause different voltage- $[Ca^{2+}]_i$ ratios for various stimulus velocities. The variability of the responses would then lead to linear voltage- $[Ca^{2+}]_i$ relationships for each velocity (e.g., 2 Hz in Fig. 4(B)), but to a deviation from linearity when pooled across different velocities (as seen in Fig. 5). In principle, this scenario requires calcium influx through ligand-gated channels, which has been proposed by a recent simulation study in another type of lobula plate neuron (Borst and Single, 2000). An alternative mechanism, relying solely on voltage-gated calcium influx, could involve a gating mechanism in calcium channels that is sensitive to local membrane potential oscillations. As stated above, such oscillations have been postulated from electrophysiological measurements and model calculations to occur at the temporal frequency of the motion stimulus and its first harmonic (Egelhaaf et al., 1989) and have been observed experimentally by Ca^{2+} -imaging of small dendritic regions (Single and Borst, 1998). If local membrane potential fluctuations were too fast for the calcium current to follow, for example due to a low-pass gating characteristic, calcium accumulation would be attenuated at high temporal frequencies. In order to distinguish between the two suggested possibilities, further experiments will have to reveal the pharmacological identity and biophysical properties of the calcium channels and transport mechanisms.

In summary, the voltage- $[Ca^{2+}]_i$ relationships of the two cell classes differ in slope, both in their positive and negative branches. To our knowledge, the present study of CH- and HS-cells is the first example of a voltage- $[Ca^{2+}]_i$ relationship measured *in vivo* and in response to sensory stimulation. Thus, they represent an example of how differing voltage-dependencies of calcium influx contribute to transform an input signal, which cannot be distinguished on the systems level (Kondoh et al., 1995), into a chemical signal with an altered stimulus-dependency, such as a different velocity tuning. In spite of being components of the same physiological response, the properties of chemical and electrical response components may differ considerably. Therefore, both components need to be studied to understand dendritic integration of synaptic input.

We thank J. Schmitz for helpful remarks on the manuscript.

REFERENCES

- Blaustein MP, Lederer WJ. 1999. Sodium/calcium exchange: its physiological implications. *Physiol Rev* 79: 763–854.
- Borst A, Egelhaaf M. 1992. In vivo imaging of calcium accumulation in fly interneurons as elicited by visual motion stimulation. *Proc Natl Acad Sci USA* 89:4139–4143.
- Borst A, Egelhaaf M. 1994. Dendritic processing of synaptic information by sensory interneurons. *TINS* 17:257–263.
- Borst A, Egelhaaf M, Haag J. 1995. Mechanisms of dendritic integration underlying gain control in fly motion-sensitive interneurons. *J Comput Neurosci* 2:5–18.
- Borst A, Haag J. 1996. The intrinsic electrophysiological characteristics of fly lobula plate tangential cells: I. Passive membrane properties. *J Comput Neurosci* 3:313–336.
- Borst A, Single S. 2000. Local current spread in electrically compact neurons of the fly. *Neurosci Lett* 285:123–126.
- Brotz TM, Borst A. 1996. Cholinergic and GABAergic receptors on fly tangential cells and their role in visual motion detection. *J Neurophysiol* 76:1786–1799.
- Dürr V. 1998. Dendritic calcium accumulation in visual interneurons of the blowfly. [Doctoral Dissertation]. Bielefeld, Germany: University of Bielefeld.
- Dürr V, Egelhaaf M. 1999. In vivo calcium accumulation in presynaptic and postsynaptic dendrites of visual interneurons. *J Neurophysiol* 82:3327–3338.
- Eckert H, Dvorak DR. 1983. The centrifugal horizontal cells in the lobula plate of the blowfly, *Phaenicia sericata*. *J Insect Physiol* 29:547–560.
- Egelhaaf M, Borst A. 1989. Transient and steady-state response properties of movement detectors. *J Opt Soc Am* 6A:116–127.
- Egelhaaf M, Borst A. 1993. A look into the cockpit of the fly: Visual orientation, algorithms, and identified neurons. *J Neurosci* 13:4563–4574.
- Egelhaaf M, Borst A. 1995. Calcium accumulation in visual interneurons of the fly: stimulus dependence and relationship to membrane potential. *J Neurophysiol* 73:2540–2552.
- Egelhaaf M, Borst A, Pilz B. 1990. The role of GABA in detecting visual motion. *Brain Res* 509:156–160.
- Egelhaaf M, Borst A, Reichardt W. 1989. Computational structure of a biological motion-detection system as revealed by local detector analysis in the fly's nervous system. *J Opt Soc Am* 6A:1070–1087.
- Egelhaaf M, Borst A, Warzecha A-K, Flecks S, Wildemann A. 1993. Neural circuit tuning fly visual interneurons to motion of small objects. II. Input organization of inhibitory circuit elements revealed by electrophysiological and optical recording techniques. *J Neurophysiol* 69:340–351.
- Egelhaaf M, Grewe J, Warzecha A-K, Kern R. 2000. Performance of a fly motion sensitive neuron under outdoors luminance conditions. *Zoology* 103 Supplement III (DZG 93.1): 64.
- Egelhaaf M, Hausen K, Reichardt W, Wehrhahn C. 1988. Visual course control in flies relies on neuronal computation of object and background motion. *TINS* 11:351–358.
- Gauck V, Egelhaaf M, Borst A. 1997. Synapse distribution on VCH, an inhibitory, motion-sensitive interneuron in the fly visual system. *J Comp Neurol* 381:489–499.
- Gilbert C. 1990. Membrane conductance changes associated with the response of motion sensitive insect visual neurons. *Z Naturforsch C* 45:1222–1224.
- Haag J, Borst A. 2000. Spatial distribution and characteristics of voltage-gated calcium signals within visual interneurons. *J Neurophysiol* 83:1039–1051.
- Hausen K. 1976. Functional characterization and anatomical identification of motion sensitive neurons in the lobula plate of the blowfly *Calliphora erythrocephala*. *Z Naturforsch* 31:629–633.
- Hausen K. 1981. Monocular and binocular computation of motion in the lobula plate of the fly. *Verh Dt Zool Ges* 1981:49–70.
- Hausen K. 1982a. Motion sensitive interneurons in the optomotor system of the fly. I. The horizontal cells: Structure and signals. *Biol Cybern* 45:143–156.
- Hausen K. 1982b. Motion sensitive interneurons in the optomotor system of the fly. II. The horizontal cells: receptive field organisation and response characteristics. *Biol Cybern* 46:67–79.
- Hausen K, Wehrhahn C. 1989. Neural circuits mediating visual flight control in flies. I. Quantitative comparison of neural and behavioural response characteristics. *J Neurosci* 9:3828–3836.
- Hausen K, Wehrhahn C. 1990. Neural circuits mediating visual flight control in flies. II. Separation of two control systems by microsurgical brain lesions. *J Neurosci* 10: 351–360.
- Hausen K, Wolburg-Buchholz K, Ribi WA. 1980. The synaptic organization of visual interneurons in the lobula complex of flies. *Cell Tissue Res* 208:371–387.
- Kondoh Y, Hasegawa Y, Okuma J, Takahashi F. 1995. Neural computation of motion in the fly visual system: quadratic nonlinearity of responses induced by picrotoxin in the HS and CH cells. *J Neurophysiol* 74:2665–2684.
- Kostyuk PG. 1992. Calcium Ions in Nerve Cell Function. Oxford: Oxford University Press. p. 1–220.
- Kurtz R, Dürr V, Egelhaaf M. 2000. Dendritic calcium accumulation associated with direction-selective adaptation in visual motion-sensitive neurons in vivo. *J Neurophysiol* 84:1914–1923.
- Maddess TL, Laughlin SB. 1985. Adaptation of the motion-sensitive neuron H1 is generated locally and governed by contrast frequency. *Proc R Soc London, B* 225:251–275.
- Ogawa H, Baba Y, Oka K. 1996. Dendritic Ca²⁺ response in cercal sensory interneurons of the cricket *Gryllus bimaculatus*. *Neurosci Lett* 219:21–24.
- Regehr WG, Tank DW. 1994. Dendritic calcium dynamics. *Curr Opin Neurobiol* 4:373–382.
- Single S. 1998. Mechanismen und Funktion dendritischer Kalziumsignale in visuellen Interneuronen der Fliege.

- [Doctoral Dissertation]. Germany: University of Tübingen.
- Single S, Borst A. 1998. Dendritic integration and its role in computing image velocity. *Science* 281:1848–1850.
- Single S, Haag J, Borst A. 1997. Dendritic computation of direction selectivity and gain control in visual interneurons. *J Neurosci* 17:6023–6030.
- Sobel EC, Tank DW. 1994. In vivo calcium dynamics in a cricket auditory neuron: an example of chemical computation. *Science* 263:823–827.
- Tank DW, Regehr WG, Delaney KR. 1995. A quantitative analysis of presynaptic calcium dynamics that contribute to short-term enhancement. *J Neurosci* 15:7940–7952.
- Vranesic I, Knöpfel T. 1991. Calculation of calcium dynamics from single wavelength fura-2 fluorescence recordings. *Pflügers Arch* 418:184–189.
- Warzecha A-K, Egelhaaf M, Borst A. 1993. Neural circuit tuning fly visual interneurons to motion of small objects. I. Dissection of the circuit by pharmacological and photoinactivation techniques. *J Neurophysiol* 69:329–339.